



HAL
open science

Scalable high-precision tuning of miniature photonic resonators by resonant cavity-enhanced photoelectrochemical etching

Eduardo Gil-Santos, Christopher Baker, Aristide Lemaître, Sara Ducci, Carmen Gomez, Giuseppe Leo, Ivan Favero

► To cite this version:

Eduardo Gil-Santos, Christopher Baker, Aristide Lemaître, Sara Ducci, Carmen Gomez, et al.. Scalable high-precision tuning of miniature photonic resonators by resonant cavity-enhanced photoelectrochemical etching. *Nature Communications*, 2017. hal-03449022

HAL Id: hal-03449022

<https://cnrs.hal.science/hal-03449022v1>

Submitted on 25 Nov 2021

HAL is a multi-disciplinary open access archive for the deposit and dissemination of scientific research documents, whether they are published or not. The documents may come from teaching and research institutions in France or abroad, or from public or private research centers.

L'archive ouverte pluridisciplinaire **HAL**, est destinée au dépôt et à la diffusion de documents scientifiques de niveau recherche, publiés ou non, émanant des établissements d'enseignement et de recherche français ou étrangers, des laboratoires publics ou privés.

Scalable high-precision tuning of miniature photonic resonators by resonant cavity-enhanced photoelectrochemical etching

EDUARDO GIL-SANTOS,¹ CHRISTOPHER BAKER,¹ ARISTIDE LEMAÎTRE,² SARA DUCCI,¹ CARMEN GOMEZ,² GIUSEPPE LEO,¹ AND IVAN FAVERO^{1,*}

¹ Matériaux et Phénomènes Quantiques, Université Paris Diderot, CNRS UMR 7162, Sorbonne Paris-Cité, 10 rue Alice Domon et Léonie Duquet, 75013 Paris, France

² Laboratoire de Photonique et de Nanostructures, Route de Nozay, CNRS, 91460 Marcoussis, France

*Corresponding author: ivan.favero@univ-paris-diderot.fr

Photonic lattices consisting of multiple mutually interacting indistinguishable cavities are a conceptual cornerstone of collective phenomena in optics, and could become central in advanced optical sensing devices. However the disorder induced by current fabrication technologies hinders the development of such resonant architectures, especially with miniature cavities. Here we present a simple and scalable method that enables efficient tuning of multiple micro- and nanophotonic resonators in collective configurations. This new method introduces the principle of cavity-enhanced photo-electrochemical etching, a resonant process triggered by light of frequency below the cavity material bandgap that allows for tremendous gains in precision and selectivity. With this approach, the resonant optical wavelength of single and multiple cavities is tuned at the picometer level, corresponding to an effective sub atomic monolayer control of their dimensions, with no quality factor degradation. The natural scalability of the process enables us to spectrally align an ensemble of high-Q cavities in a permanent manner, overcoming the dimension variability resulting from nanofabrication. The technique is introduced on a gallium arsenide nanophotonic platform, and illustrated by finely tuning one, two, and up to five resonators, both in air and in liquid. It opens the way to multiple applications, like the fabrication of large networks of identical coupled resonators or the referencing of chip-based cavities to external etalons.

The advent of micro- and nanofabrication techniques has had a profound impact on the control of light-matter interactions, be it in semiconductor, metallic or dielectric materials. It is today possible to tailor the optical properties of emitters by engineering their coupling to solid-state resonant cavities, waveguides or antennas. Collective photonic architectures based on micro- and nanoscale resonators serve in great many contexts like information processing [1-3], sensing [4], metamaterials [5], polaritonics [6], non-linear optics [7], optomechanics [8] and plasmonics [9]. Lattices of resonant cavities are also becoming a test-bed for the physics of strongly correlated optical systems [10], with a recent focus on synchronization [11], phase-transition [12] and topological phenomena [13]. However, in all these frontier applications, there is still a gap between ideas and experimental realizations, due to insufficient deterministic control in the resonant optical

wavelength of single and multiple resonators, which precludes many of the above concepts to become reality. Technologically speaking, conventional nanofabrication tools like electronic beam lithography or ion milling and etching typically allow for a nanometer-scale precision in the finished device's dimensions at best. For micro- and nanoscale cavities, such an imprecision translates into a sizable uncertainty in the resonant optical wavelength. As an example, let us consider a whispering gallery mode (WGM) disk resonator of nominal radius $R=1\mu\text{m}$, fabricated out of a strongly refractive semiconductor like Gallium Arsenide (GaAs), and resonating at a wavelength $\lambda_{\text{WGM}} \approx 1\mu\text{m}$ [14,15]. Since $\delta\lambda_{\text{WGM}}/\lambda_{\text{WGM}}=\delta R/R$ [14], with δR the radius imprecision, the near-infrared optical modes of such disk, once fabricated, also face an imprecision $\delta\lambda_{\text{WGM}}$ of a few nanometers in their resonance. For two resonators to share a common resonance frequency, a precision $\delta R < R/Q$ is required, with Q the resonator quality factor. Even with a modest $Q=10^4$, this means a resonator size control at the level of the Angstrom, the level of a single atom. In consequence, two nominally identical cavities, once fabricated, always resonate at distinct wavelengths, precluding collective spectral alignment or resonant interaction with targeted references. This disorder is a major obstacle for the future of nanophotonics. It needs to be overcome, ideally with a technique simple enough to spread from basic research experiments to industrial settings, where complex photonic architectures will demand reasonable technological complexity in the handling.

Techniques have been proposed to partially address these issues. Gas adsorption and surface desorption and oxidation allowed for example tuning individual miniature optical resonators [16-21]. Thermal [22,11], electrical [23,24] and mechanical [25] tuning of optical micro-resonators was also demonstrated, but requires continuous energy consumption. These approaches produce non-permanent effects and are not sufficiently scalable. The tuning of photonic structures was obtained as well by functionalization with a photochromic film [26], a laser-addressable polyelectrolyte [27] or a photosensitive layer [28]. However, these techniques complicate the handling of multiple cavities and tend to degrade optical and mechanical properties by surface modification. Ultra-violet light at or above the bandgap was used to photo-etch gallium nitride devices [29-31] and trim silicon optical structures [32], however with limited precision. Fluidic tuning was achieved by water infiltration and evaporation at the level of individual photonic cavities, but with little permanence [33]. Importantly, all of these methods are poorly scalable.

Here we present a new method to achieve spectral tuning of micro- and nanophotonic resonant cavities, which solves all of the above shortcomings. The method introduces the concept of *resonant cavity-enhanced* photo-electrochemical (PEC) etching, whereby the dielectric material forming the optical cavity is etched only in the presence of light resonating in the cavity and when immersed in a fluid. In contrast to conventional PEC configurations that use light above the bandgap, this new technique operates in the transparency region of the material. This latter fact enables taking advantage of the high- Q resonances of the cavities to be tuned. When a cavity is driven at resonance by a laser, a strong internal light-enhancement takes place and triggers an enhanced etching selectively within the cavity, leading to its tuning. An illustration of such a situation is given in Fig. 1(a), where one individual resonator is selectively etched and tuned, while the other two are out of

resonance and remain in essence unaffected (see Supplementary Information for a detailed discussion). The technique can operate with a single laser, produces permanent results with no optical performance degradation, and is automatically scalable to multiple resonators. It is both site-specific, in that it resonantly addresses each individual resonator of an inhomogeneous ensemble, and collective, because it does not require individual identification of each resonator to achieve spectral alignment of the ensemble. Being adjustable by light intensity, it allows both fine-tuning of a resonator's wavelength at a picometer level, and coarse-tuning over tens of nanometers, both within a few minutes of time and with little power consumption. Here we introduce the technique on a Gallium Arsenide photonic platform, a material that allows resonant PEC etching in water. To establish the performance of the method, we investigate first the tuning of an individual resonator, and then demonstrate the collective tuning of an ensemble of five semiconductor photonic cavities immersed in liquid water. We finally extend the technique to a simple humid atmosphere, showing that versatility in application of the method is obtainable with alleviated fluidic constraints.

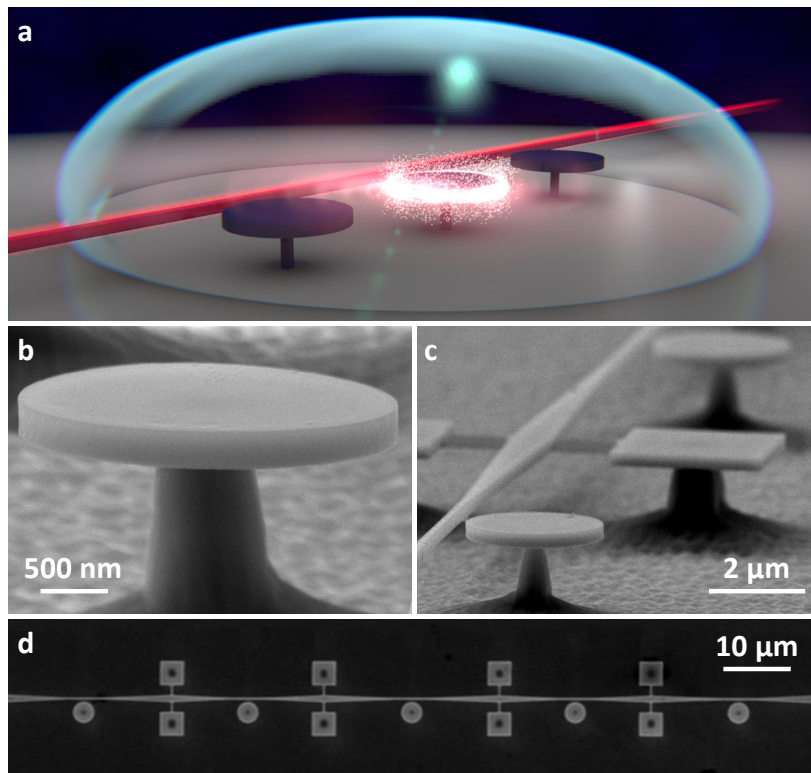


Fig. 1. Resonant PEC tuning of GaAs disk resonators on a chip. (a) Illustration of the resonant PEC etching of a disk resonator coupled to a linear optical waveguide. Laser light is in red while the shining zone represents a whispering gallery mode where electromagnetic energy localizes and triggers the cavity etching. The disk belongs to a set of three resonators immersed in a fluid droplet. (b) Side-view electron micrograph of a single GaAs disk positioned atop a central AlGaAs pedestal. (c) Set of 2 disks positioned along a common GaAs suspended optical waveguide. The waveguide's tapered parts lie close to the disks while square-shape anchors support its widest part. (d) Top-view electron micrograph of five disk resonators in series along a waveguide held by 8 square-shape anchors.

The results reported in the following are obtained with GaAs disk resonators, whose typical dimensions are of 320 nm in thickness and 1 μm in radius [34-36]. These resonators can support WGMs of mode volume smaller than $1\mu\text{m}^3$, and represent

archetypes of micro/nano photonic cavities for the purposes discussed here. Since PEC processes occur in many dielectric semiconductors, the method of resonant cavity-enhanced PEC tuning introduced here with GaAs is in principle transposable to other material platforms. For the case of silicon, the water-rich fluidic environment used in this work shall be replaced by a fluoride-based liquid or vapor to adapt the technique [37]. The method is in essence adaptable as well to different photonic cavity architectures, for example those based on photonic crystals, rings or slots.

Our disk resonators are isolated from the substrate through an Aluminum Gallium Arsenide (AlGaAs) pedestal, as shown in Fig. 1(b). They are fabricated out of a GaAs (320 nm)/Al_{0.8}Ga_{0.2}As (1800 nm)/GaAs epitaxial wafer, by electron beam lithography, non-selective inductively coupled plasma reactive ion etching, and selective under-etching in a dilute hydrofluoric acid solution. GaAs waveguides integrating a taper with nanoscale transverse dimensions allow evanescent optical coupling of light into the disk's WGMs [38], and are suspended in the resonator's vicinity (see Fig. 1(c) and (d)). Thanks to the large refractive index of GaAs, the chip can be immersed in a transparent liquid while preserving the confinement and guiding of light in the resonators and waveguides. The presence of a microliter droplet of liquid covering many resonators still allows optical evanescent coupling disk/waveguide experiments to be performed in-situ [39,40]. This is the first approach that we employ to tune our disk resonators by resonant cavity-enhanced PEC (see Supplementary Information for set-up details). The disk WGMs appear as resonant dips in the waveguide's optical transmission spectrum (see Fig. 2(a)). In Fig. 2(a), the linewidth of both visible resonances is 32 pm in ambient conditions before liquid immersion, corresponding to a loaded WGM quality factor Q of 41 000. At resonance, the light-assisted PEC etching of the cavity is resonantly favored over the etching of the waveguide (see Supplementary Information). The etching reduces the size of the disk resonator and blue shifts its optical resonances. This shift can be continuously controlled and monitored in time in the liquid, by continuously sweeping the laser wavelength over the resonance. A real-time video of such continuous monitoring is shown in Supplementary Video S1 of the Supplementary Information. Once the desired amount of etching is reached, the laser is switched-off and the sample dried. The dry resonator's optical spectrum, whose overall structure is preserved, reveals a permanent blue shift of 4 nm (see Fig. 2(b)). The linewidth of the two resonances is now of 19 and 25 pm respectively, with an almost unaltered contrast. The loaded Qs rise to 70 000 and 52 000, which represents a marked reduction of optical losses with respect to the situation before etching. We carried out similar tests on many resonators, showing that the optical Q is sometimes improved by the resonant cavity-enhanced PEC tuning, and is at least never degraded. Let us now discuss the mechanisms at play in our tuning technique that are responsible for these advantageous features.

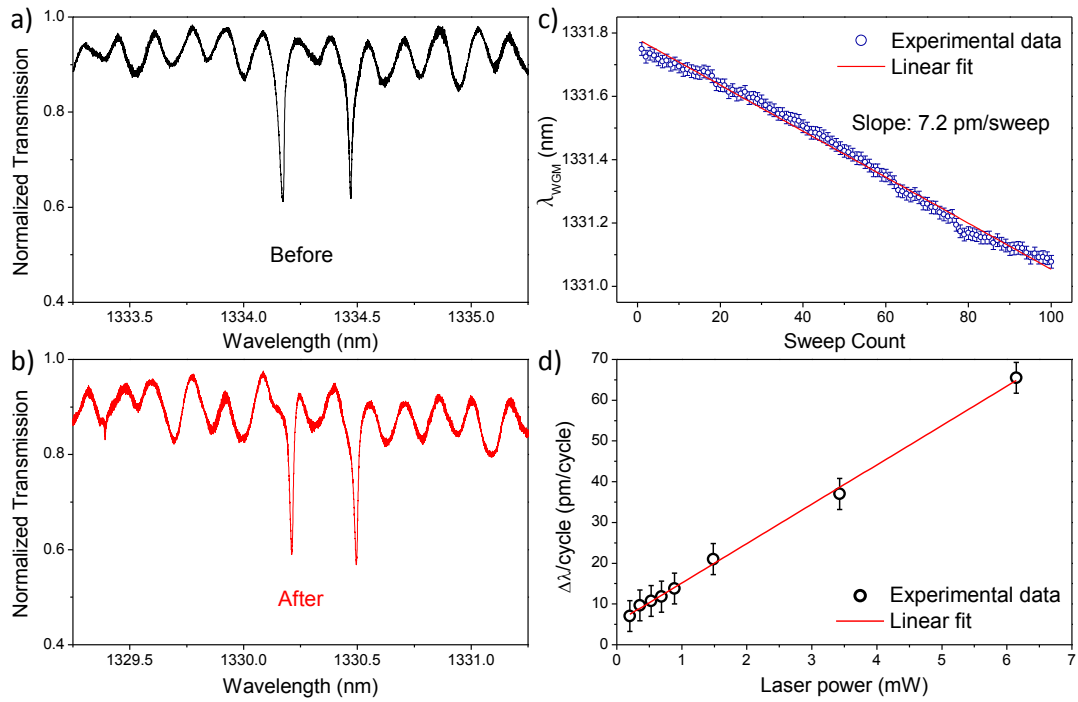


Fig. 2. Resonant PEC tuning of a single GaAs WGM disk resonator. (a) Optical spectrum before resonant PEC etching, with a doublet associated to two normal modes of the disk, consisting of a mixture of clockwise and counter-clockwise WGMs [15]. (b) Optical spectrum after 4 nm of resonant PEC etching. The low-contrast oscillations are residual interferences produced by reflections at the waveguide input and output facets. They can be mitigated by proper guide design. (c) Wavelength tuning of the WGM of a GaAs disk resonator by subsequent cycles of PEC etching at low optical power, reaching picometer precision. This translates into an etch speed of 0.5-1 nm/s for a continuous dropped power of 1 μ W in the cavity WGM. (d) Wavelength tuning per cycle (see text) as a function of the laser optical output power, which is proportional to the optical power guided in the coupling waveguide. Each point has been obtained by averaging over 100 cycles.

In standard (non-resonant) PEC etching one optically pumps, above the bandgap, a semiconductor immersed in an electrically conductive liquid. Ultra-violet light is generally used to generate carriers and lead to the formation of ionic species of the semiconductor. The latter are dissolved in the presence of ions provided by the electrolyte liquid [41-43]. The associated chemical reaction for GaAs reads $\text{GaAs} \rightarrow \text{Ga}^{3+} + \text{As}^{3-} + 6e^-$, whose products form oxides with the hydroxyde ions of water and are then removed [41]. In the present work in contrast, we achieve resonant PEC etching with light of frequency in the transparency region of the material. The reason is that high-Q GaAs disk resonators, just as all equivalent high-Q photonic cavities, can absorb a (small) fraction of the resonating light they store at resonance. In GaAs disks, a residual linear absorption is for example caused by mid-gap states localized at the resonator's surface [40]. In consequence, the ionic species required for triggering the PEC etching can be generated while optically pumping below the material bandgap, at the resonance of a WGM. This *resonant cavity-enhanced* nature of our PEC tuning brings in key advantages. For example it leads to high spatial selectivity by favoring the etching precisely within the optical mode of the selected resonator. This spatial localization of the process has several beneficial consequences: in the case of a WGM localized at the periphery of a

disk, it may be responsible for the Q improvement observed in our experiments, by smoothing out geometric irregularities of the disk contour. Another benefit is that a small flux of light can be used to etch each resonator, allowing a high level of control in the amount of tuning, and hence a high tuning precision. This is exemplified in Fig. 2(c), which demonstrates the spectral accuracy of the resonant PEC technique by employing a series of elementary fine-tuning cycles. Each cycle consists in rapidly sweeping the wavelength of the laser back and forth over the WGM resonance, which allows for both acquiring an optical spectrum and step tuning the resonating wavelength. Fig. 2(c) shows a resonance wavelength measured on a GaAs disk WGM, as a function of the number of applied cycles. The evolution is linear in the number of cycles, with a blue shift of 7.2 pm per cycle. For the disk considered above, and translated into an effective change of radius, this represents a size control with a precision of 8pm per cycle, which is well below the material's interatomic distance. More precisely, each of these sweep cycles reduces the disk's size by less than a 30th of an atomic monolayer (280 pm). In contrast, the simple process of immersing the chip in an acidic solution to remove the native surface oxide would shift the WGM optical resonance by approximately 2 nm [40,44]. The sweep-cycle tuning procedure outlined here is more than 250 times more precise. By calculating the effective etching duration per cycle, we evaluate an etching speed of 0.5-1 nm of radius change per second, for 1 μ W of continuous optical power dropped into the cavity WGM. By increasing the laser power, one can adjust the amount of tuning per cycle in a linear fashion, as shown in Fig. 2(d). Note that the intercept of the linear fit does not cross the origin, which is mainly ascribed to a very slow non-selective GaAs etching in water (see discussion below and Supplementary Information). By choosing the light intensity and the number of cycles, the resonance wavelength can be tuned between a few picometers and several tens of nanometers, with permanent results, and within just a few minutes. Important is to note that the sweep-cycle mode is not the only procedure that can be used for tuning. Another possibility is to have the laser wavelength continuously following the optical resonance as it is tuned. At low optical power, our experiments indicate that this latter procedure leads to a tuning precision even better than the picometer, currently beyond the spectral accuracy at our disposal in the laboratory. This great spectral versatility of the technique in terms of tunability and precision also comes with other benefits when ensembles of resonating cavities are handled, as we discuss now in more detail.

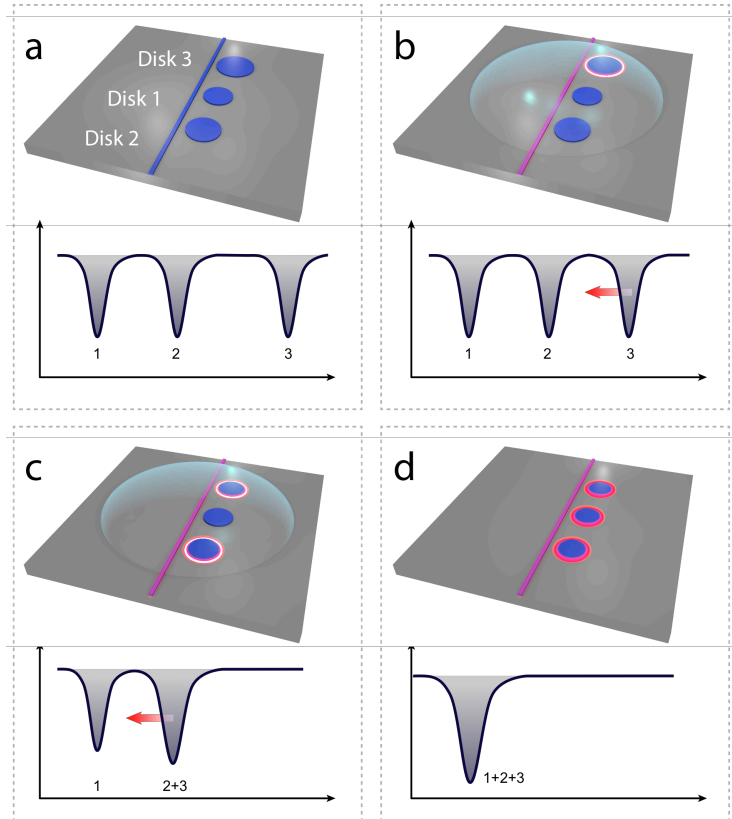


Fig. 3. Scalability of the resonant cavity-enhanced PEC tuning explained for the case of three cavities in series. The illustrated spectra represent the optical transmission as a function of wavelength. a) An optical bus waveguide couples in series to three disk cavities having distinct radius, hence distinct optical resonance. The optical spectrum consists of three resonances. b) The cavities are immersed in a PEC fluid and the laser wavelength is set to the largest resonant wavelength. This triggers resonant PEC etching in the disk of largest radius (disk 3), progressively reducing its radius and its resonant wavelength. c) When disk 3 becomes resonant with disk 2, the resonant cavity-enhanced PEC etching becomes concomitant in these two disks, and displaces their optical resonance towards that of the smallest disk of the set (disk 1). d) At a certain point, disks 2 and 3 become resonant with disk 1, providing us with a set of three spectrally aligned cavities.

Indeed one crucial aspect of the method is its natural scalability, which is obtained with a single laser and with relatively modest efforts. The scalability is a consequence of the *resonant* nature of our cavity-enhanced tuning process, and is easily understood in the case of three resonators (see Fig 3). Let us imagine three distinct disk resonators (1,2,3) of increasing radius, hence increasing resonant wavelength (Fig. 3(a)). Let us immerse them in a PEC enabling fluid, and set the laser at resonance with disk 3 (Fig. 3(b)). The cavity-enhanced PEC etching starts preferentially in disk 3 and reduces its radius. As its resonant wavelength gets in consequence blue-shifted, we continuously and slowly sweep the laser towards smaller wavelengths in order to track the resonance and sustain the etching, until disk 3 adopts the resonant wavelength of disk 2. From that moment on, disk 2 and 3 get resonantly etched together by the laser, and are progressively tuned to lower wavelength (Fig. 3(c)). When their common resonant wavelength reaches that of disk 1, the three disk resonators are spectrally aligned (Fig. 3(d)). The principles of this scalable tuning can be extended to a larger number of resonators, using a single laser and a single laser wavelength sweep, and they enable collective spectral alignment without having to individually identify each resonator of the set (i.e. the tuning procedure remains the same irrespective of the order of disks 1,2,...,N along

the waveguide). This is in strong contrast with all other tuning methods investigated so far. While the case of three resonators is used for illustrative purposes in Fig. 3 (see also Supplementary Information), below we experimentally demonstrate the scalability of the process with five cavities.

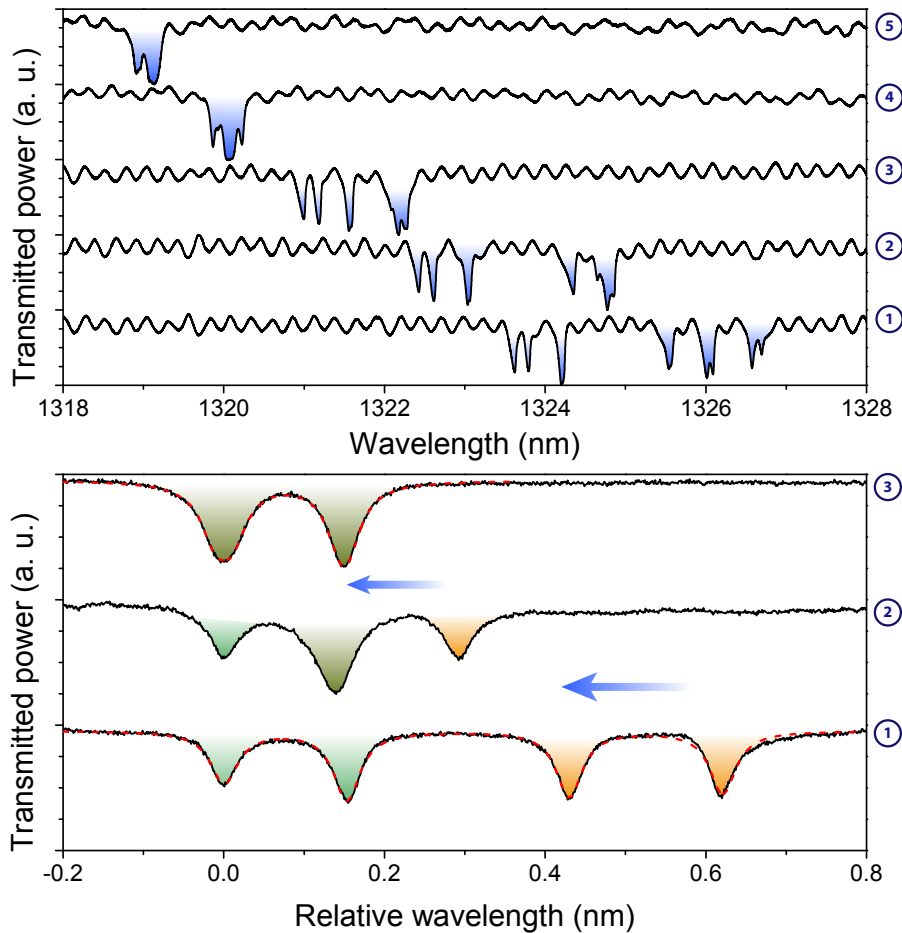


Fig. 4. Collective tuning of photonic resonators by resonant cavity- enhanced PEC etching. Upper panel: Optical spectra corresponding to step-by-step spectral alignment of five WGM resonators in liquid water (see text for details). In the first spectrum, the five resonators (1 to 5) appear in order of their resonant wavelength ($\lambda_1 < \dots < \lambda_5$). On top of the spectral merging of the five resonators, a residual non-selective etching is also present and discussed in full in the Supplementary Information. Lower panel: Spectral tuning of two WGM resonators, performed directly in humid air in absence of liquid. In these latter spectra, relative wavelengths are displayed, with the origin being set by the smallest wavelength of the group of resonances. Indeed, since the resonant cavity-enhanced PEC tuning in humid air is a slow process, we removed here the contribution of slow temperature variations in the laboratory, which typically red-shift all wavelengths by 200 picometers for 1°C of temperature variation (see Supplementary Information for extra raw data).

The upper panel of Fig. 4 shows a series of five optical spectra acquired on a set of five distinct disks placed along a common optical coupling waveguide in the configuration of Fig. 1(d), and immersed in liquid water. The first spectrum (step 1) contains five groups of resonances, each group being associated to a distinct disk. Three groups display a clearly visible doublet structure, while this structure is not clearly resolved in the two others. Even though the five disks are nominally the same, they optically resonate at distinct wavelengths ($\lambda_1 < \dots < \lambda_5$), because of nanofabrication disorder. In the case shown here, the largest disk (disk 5) resonates at the largest wavelength λ_5 , around 1326.8 nm. By setting the laser to this

wavelength, we trigger the resonant PEC etching preferentially in disk 5 and consequently blue shift its resonances. We track these resonances by continuously adjusting the laser wavelength to them, in order to sustain the etching of disk 5, until it spectrally aligns with disk 4. A second spectrum is then acquired (step 2), revealing the obtained relative shift of the resonances of disk 5. At step 2, disk 5's resonances are spectrally overlapped to those of disk 4, the second largest disk at the beginning of the procedure. From that stage on, the laser etches disks 5 and 4 concomitantly, and spectrally drags their aligned resonances towards those of disk 3. At step number 3, the resonances of disks 5 and 4 consequently merge with that of disk 3, and the laser now starts etching these three disks together. The procedure of tuning and spectrum acquisition is repeated this way, progressively bringing all the disks to spectrally align. At step 5, the five disks have their resonances spectrally overlapped, and the laser can be switched off. On top of this spectral overlap, we observe that a non-selective tuning takes place along the procedure, generating an additional blue shift of the set of resonances. The origin of this non-selective tuning is discussed in details in the Supplementary Information, and it can be mitigated if required for a specific application. The final result of the tuning procedure is a set of five spectrally aligned cavities. Important is to note that, while five steps are discussed in the upper panel of Fig. 4 in order to illustrate the process, the PEC spectral alignment can also be performed by a single slow continuous laser sweep starting from the red detuned side of resonances. This continuous collective tuning mode is illustrated by a simulation in Supplementary VideoS2 in the Supplementary Information.

While PEC tuning in a liquid like demonstrated above may suffice in a number of applications, the constraints associated to liquid immersion may pose problems for some cavity geometries and for some photonic materials. For this reason, in the lower panel of Fig. 4, we extend the method to a gaseous environment, and circumvent liquid immersion. With GaAs, the humidity of ambient air is sufficient to trigger a very slow PEC etching process under resonant optical pumping of the cavity. At equal pumping power, we have evaluated that in this latter case the etching speed is six orders of magnitude slower than in water. Intermediate speeds can be obtained by controlling the water content of the enviroing atmosphere. The lower panel of Fig. 4 shows the spectral tuning of two distinct GaAs disk resonators under ambient humidity conditions, in the configuration of Fig. 1(c). At step 1, we observe two groups of doublets, each group being associated to a given disk. At the intermediate step 2, these resonances partially overlap. At the final step (step 3), the two doublets are perfectly overlapped. The two disks are now, once and for all, resonating at the same optical wavelength down to a precision better than 10 pm. The dashed lines are a fit provided by a simple model of cascaded resonators coupled to a common optical waveguide, and support that the tuning procedure follows the principles introduced above. With the slow speed of etching reached in these conditions, the tuning procedure becomes time consuming (10 hours of experiments here), but it allows a level of spectral control that is even superior to the picometer precision reached in the liquid in Fig. 2. For each specific application, a compromise between precision and speed will need to be made, by adjusting the density of ionic species in the fluid environment (liquid or gas) used to sustain the PEC processes.

The collective tuning method can be naturally scaled to more than five resonators, again because spectral alignment does not require singling out each resonator. The precision and selectivity of the method can be improved as well beyond what we report here. As detailed in the Supplementary Information, the tuning precision of a few picometers reached in water in the sweep-cycle mode is, in our case, set by the absolute spectral inaccuracy of our laser, and could be improved by improved laser referencing. The selectivity is limited by residual non-selective tuning that could be mitigated as well (see Supplementary Information). Since we observed resonant PEC etching of GaAs disks in ammonia and isopropanol as well, we know that other ionic liquids can be employed to gain even better control on the technique. As demonstrated by our tuning experiments in humid air, we also understand that controlled ionic gas atmospheres will enable extension of the method to many other cases. Specific optimization will be needed for each semiconductor showing capability of PEC etching, like silicon, gallium-nitride or antimonide, zinc-sulfide or selenide, to name a few. But overall, because the resonant PEC etching method is site-specific, precise, naturally collective, and gives permanent effects, it may become a powerful tool for nanoscale photonic devices, and motivate extensions to many materials and structures. The field of nanophotonics will need many advances of the kind to hold its great promises of new science and applications.

Acknowledgments

This work was supported by the European Research Council through the Ganoms project.

Author contributions

E. G. L and C. B conducted experiments and analyzed the results with I. F. C. G and A. L grew the epitaxial material. All authors discussed the method and wrote the manuscript.

The authors declare no competing financial interest.

References

1. J. K. Poon, L. Zhu, G. A. DeRose, and A. Yariv. Polymer Microring Coupled-Resonator Optical Waveguides. *Opt. Lett.* **31**, 456 (2006).
2. M. T. Hill, H. J. S. Dorren, T. de Vries, X. J. M. Leijtens, J. H. den Besten, B. Smalbrugge, Y. S. Oei, H. Binsma, G. D. Khoe, and M. K. Smit. A fast low-power optical memory based on coupled micro-ring lasers. *Nature* **432**, 206 (2004).
3. F. Xia, L. Sekaric, and Y. Vlasov. Ultracompact optical buffers on a silicon chip. *Nature Photonics* **1**, 65 (2006).
4. A. L. Washburn, M. S. Luchansky, A. L. Bowman and R. C. Bailey. Label-free, multiplexed biomolecular analysis using arrays of silicon photonic microring resonators. *Anal. Chem.* **82** (1), 69 (2010).
5. V. M. Shalaev. Optical negative-index metamaterials. *Nature Photonics* **1**, 41 - 48 (2007).

6. T. Jacqmin, I. Carusotto, I. Sagnes, M. Abbarchi, D. Solnyshkov, G. Malpuech, E. Galopin, A. Lemaître, J. Bloch, A. Amo. Direct Observation of Dirac Cones and a Flatband in a Honeycomb Lattice for Polaritons. *Phys. Rev. Lett.* **112**, 116402 (2014).
7. A. Le Boité, G. Orso, and C. Ciuti. Steady-State Phases and Tunneling-Induced Instabilities in the Driven Dissipative Bose-Hubbard Model. *Phys. Rev. Lett.* **110**, 233601 (2013).
8. G. Heinrich, M. Ludwig, J. Qian, B. Kubala, and F. Marquardt. Collective dynamics in optomechanical arrays. *Phys. Rev. Lett.* **107**, 043603 (2011).
9. Z. Liu, A. Boltasseva, R. H. Pedersen, R. Bakker, A. V. Kildishev, V. P. Drachev, V. M. Shalaev. Plasmonic nanoantenna arrays for the visible. *Metamaterials* **2**, 45 (2008).
10. I. Carusotto and C. Ciuti. Quantum fluids of light. *Rev. Mod. Phys.* **85**, 299 (2013).
11. M. Zhang, G. S. Wiederhecker, S. Manipatruni, A. Barnard, P. McEuen, and M. Lipson. Synchronization of micromechanical oscillators using light. *Phys. Rev. Lett.* **109**, 233906 (2012).
12. C. Liu, A. Di Falco, and A. Fratalocchi. Dicke Phase Transition with Multiple Superradiant States in Quantum Chaotic Resonators. *Phys. Rev. X* **4**, 021048 (2014).
13. V. Peano, C. Brendel, M. Schmidt, and F. Marquardt. Topological Phases of Sound and Light. *Phys. Rev. X* **5**, 031011 (2015).
14. L. Ding, C. Baker, P. Senellart, A. Lemaître, S. Ducci, G. Leo, and I. Favero. High frequency GaAs nano-optomechanical disk resonator. *Phys. Rev. Lett.* **105**, 26, 263903 (2010).
15. J. C. L. Ding, C. Baker, A. Andronico, D. Parrain, P. Senellart, A. Lemaître, S. Ducci, G. Leo, and I. Favero, "Gallium arsenide disk optomechanical resonators," in *Handbook of Optical Microcavities* (PanStanford, 2014).
16. K. Srinivasan and O. Painter. Optical fiber taper coupling and high-resolution wavelength tuning of microdisk resonators at cryogenic temperatures. *Appl. Phys. Lett.* **90**, 3, 031114 (2007).
17. S. Mosor, J. Hendrickson, B. C. Richards, J. Sweet, G. Khitrova, H. M. Gibbs, T. Yoshie, A. Scherer, O. B. Shchekin, and D. G. Deppe. Scanning a photonic crystal slab nanocavity by condensation of xenon. *Applied Physics Letters* **87**, 141105 (2005).
18. A. Rastelli, A. Ulhaq, S. Kiravittaya, L. Wang, A. Zrenner, and O. G. Schmidt. In situ laser microprocessing of single self-assembled quantum dots and optical microcavities. *Applied Physics Letters* **90**, 073120 (2007).
19. H. S. Lee, S. Kiravittaya, S. Kumar, J. D. Plumhof, L. Balet, L. H. Li, M. Francardi, A. Gerardino, A. Fiore, A. Rastelli, and O. G. Schmidt. Local tuning of photonic crystal nanocavity modes by laser-assisted oxidation. *Applied Physics Letters* **95**, 191109 (2009).
20. F. Intonti, N. Caselli, S. Vignolini, F. Riboli, S. Kumar, A. Rastelli, O. G. Schmidt, M. Francardi, A. Gerardino, L. Balet, L. H. Li, A. Fiore, and M. Gurioli. Mode tuning of photonic crystal nanocavities by photoinduced non-thermal oxidation. *Applied Physics Letters* **100**, 033116 (2012).

21. A. Y. Piggott, K. G. Lagoudakis, T. Sarmiento, M. Bajcsy, G. Shambat, and J. Vučković. Photo-oxidative tuning of individual and coupled GaAs photonic crystal cavities. *Optics Express* Vol. 22, Issue 12, pp. 15017-15023 (2014).
22. P. Dong, W. Qian, H. Liang, R. Shafiqi, D. Feng, G. Li, J. E. Cunningham, A. V. Krishnamoorthy, and M. Asghari. Thermally tunable silicon racetrack resonators with ultralow tuning power. *Opt. Exp.* **18**, 19, 20298 (2010).
23. J. M. Shainline, G. Fernandes, Z. Liu, and J. Xu. Broad tuning of whispering-gallery modes in silicon microdisks. *Opt. Exp.* **18**, 14, 14345 (2010).
24. Y. Shen, I. B. Divliansky, D. N. Basov, and S. Mookherjea. Electric-field-driven nano-oxidation trimming of silicon microrings and interferometers. *Opt. Lett.* **36**, 14, 2668 (2011).
25. W. von Klitzing, R. Long, V. S. Ilchenko, J. Hare, and V. Lefèvre-Seguin. Frequency tuning of the whispering-gallery modes of silica microspheres for cavity quantum electrodynamics and spectroscopy. *Opt. Lett.* **26**, 3, 166 (2001).
26. D. Sridharan, E. Waks, G. Solomon, and J. T. Fourkas. A reversibly tunable photonic crystal nanocavity laser using photochromic thin film. *Appl. Phys. Lett.* **96**, 15, 153303 (2010).
27. K. Piegdon, M. Lexow, G. Grundmeier, H.-S. Kitzerow, K. Pärschke, D. Mergel, D. Reuter, A. Wieck, and C. Meier. All-optical tunability of microdisk lasers via photo-addressable polyelectrolyte functionalization. *Opt. Exp.* **20**, 6, 6060 (2012).
28. S. Grillanda, V. Raghunathan, V. Singh, F. Morichetti, J. Michel, L. Kimerling, A. Melloni and A. Agarwal. Post-fabrication trimming of athermal silicon waveguides. *Opt. Lett.* **38**, 24, 5450 (2013).
29. N. Niu, T.-L. Liu, I. Aharonovich, K. J. Russell, A. Woolf, T. C. Sadler, H. A. El-Ella, M. J. Kappers, R. A. Oliver, and E. L. Hu. A full free spectral range tuning of p-i-n doped gallium nitride microdisk cavity. *Appl. Phys. Lett.* **101**, 16, 161105 (2012).
30. E. Trichas, M. Kayambaki, E. Iliopoulos, N. T. Pelekanos and P. G. Savvidis. Resonantly enhanced selective photochemical etching of GaN. *Appl. Phys. Lett.* **94**, 173505 (2009).
31. X. Xiao, A. J. Fischer, G. T. Wang, P. Lu, D. D. Koleske, M. E. Coltrin, J. B. Wright, S. Liu, I. Brener, G. S. Subramania, and J. Y. Tsao. Quantum-Size-Controlled Photoelectrochemical Fabrication of Epitaxial InGaN Quantum Dots. *Nano Lett.* **14** (10), 5616–5620 (2014).
32. D. Bachman, Z. Chen, R. Fedosejevs, Y. Y. Tsui and V. Van. Permanent fine tuning of silicon microring devices by femtosecond laser surface amorphization and ablation. *Opt. Exp.* **21**, 9, 11048 (2013).
33. F. Intonti, S. Vignolini, F. Riboli, M. Zani, D. S. Wiersma, L. Balet, L. H. Li, M. Francardi, A. Gerardino, A. Fiore and M. Gurioli. Nanofluidic control of coupled photonic crystal resonators. *Appl. Phys. Lett.* **96**, 141114 (2010).
34. L. Ding, C. Baker, P. Senellart, A. Lemaitre, S. Ducci, G. Leo and I. Favero. Wavelength-sized GaAs optomechanical resonators with gigahertz frequency. *Appl. Phys. Lett.* **98**, 113108 (2011).
35. D. T. Nguyen, C. Baker, W. Hease, S. Sejil, P. Senellart, A. Lemaitre, S. Ducci, G. Leo et I. Favero. Ultrahigh Q-frequency product for optomechanical disk resonators with a mechanical shield. *Appl. Phys. Lett.* **103**, 241112 (2013).

36. D. T. Nguyen, W. Hease, C. Baker, E. Gil-Santos, P. Senellart, A. Lemaître, S. Ducci, G. Leo, and I. Favero. Improved optomechanical disk resonator sitting on a pedestal mechanical shield. *New Journal of Physics* **17**, 023016 (2015).
37. C. Levy-Clement, A. Lagoubi, R. Tenne, M. Neumann-Spallart. Photoelectrochemical etching of silicon. *Electrochimica Acta* **37**, 877 (1992).
38. C. Baker, C. Belacel, A. Andronico, P. Senellart, A. Lemaitre, E. Galopin, S. Ducci, G. Leo, and I. Favero. Critical optical coupling between a GaAs disk and a nanowaveguide suspended on the chip. *Appl. Phys. Lett.* **99**, 151117 (2011).
39. E. Gil-Santos, C. Baker, D. T. Nguyen, A. Lemaître, C. Gomez, G. Leo, S. Ducci and I. Favero. High-frequency nano-optomechanical disk resonators in liquids. *Nat. Nanotech.* **10**, 810 (2015).
40. D. Parrain, C. Baker, G. Wang, A. Lemaitre, P. Senellart, G. Leo, S. Ducci and I. Favero. Origin of optical losses in gallium arsenide disk whispering gallery resonators. *Opt. Exp.* **23**, 15, 19656 (2015).
41. R. W. Hoisty. Photoetching and Plating of Gallium Arsenide. *J. Electrochem. Soc.* **108**, 790 (1961).
42. D. Greene. Preferential Photoelectrochemical Dissolution of n-GaAs in Fe (III)-Based Etches. *Inst. Phys. Conf. Ser.* **33a**, 141 (1977).
43. R. Tenne and G. Hodes. Improved efficiency of CdSe photoanodes by photoelectrochemical etching. *Appl. Phys. Lett.* **37**, 428 (1980).
44. A. Badolato, K. Hennessy, M. Atatüre, J. Dreiser, E. Hu, P. M. Petroff, and A. Imamoglu. Deterministic coupling of single quantum dots to single nanocavity modes. *Science* **308**, 5725, 1158 (2005).
-

Scalable high-precision tuning of miniature photonic resonators by resonant cavity-enhanced photoelectrochemical etching: Supplementary Information

EDUARDO GIL-SANTOS,¹ CHRISTOPHER BAKER,¹ ARISTIDE LEMAÎTRE,² SARA DUCCI,¹ CARMEN GOMEZ,² GIUSEPPE LEO,¹ AND IVAN FAVERO^{1,*}

¹ Matériaux et Phénomènes Quantiques, Université Paris Diderot, CNRS UMR 7162, Sorbonne Paris-Cité, 10 rue Alice Domon et Léonie Duquet, 75013 Paris, France

² Laboratoire de Photonique et de Nanostructures, Route de Nozay, CNRS, 91460 Marcoussis, France

Experimental set-up

Supplementary Figure S1 shows a binocular top-view of the set-up employed for the resonant PEC tuning of GaAs disk resonators.

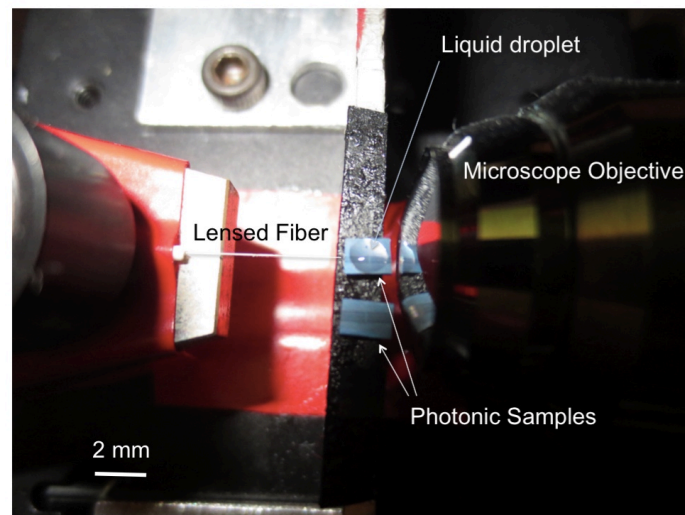


Fig. S1. Resonant PEC etching set-up. Two semiconductor photonic samples are placed on a sample holder (in black). A liquid droplet is formed on the upper sample. This latter sample is sandwiched between an optical micro-lensed fiber for light injection into the sample's waveguides (left) and a microscope objective for light collection at the waveguide's output. The lensed fiber is connected to a tunable external cavity diode laser (Tunics model, continuous-wave, mode-hop-free, line width of 400kHz) and the light collected by the objective focused back on a p-i-n photodetector. The sample holder, lensed fiber and objective are mounted on xyz micro-positioning stages for alignment.

Laser imprecision and tuning

The results shown in the main text indicate that a wavelength shift of 7,2 pm per cycle is reached in the resonant PEC tuning process, when subsequent tuning cycles are used at low laser power. This wavelength shift per cycle must be understood as a mean value, as each point of the lower panel of Fig. 3 is obtained by averaging over 100 cycles. Here we show a statistical analysis of the measured per-cycle wavelength shift, to understand the origin of the residual imprecision of our tuning method. The upper panel of Supplementary Figure S2 shows a histogram of the shift in a similar low optical power regime, derived from 100 measured cycles performed in water. This histogram shows a

mean value of 7 pm for the (negative) wavelength shift. The standard deviation of the measurement amounts to 8 pm, which sets the experimental precision of our cycle tuning mode. The lower panel of Supplementary Figure S2 shows the same analysis with the resonators operated in air, hence in absence of PEC etching. The mean value is this time zero (no etching) and the standard deviation 7 pm. This indicates that our cycle-tuning experiments are affected by an imprecision of 7pm in the measurement of the resonant wavelength λ_{WGM} . We anticipate this imprecision to be associated to a lack of continuous spectral accuracy as we sweep the laser wavelength over subsequent cycles (we use rapid sweep scans of an external cavity diode laser). While this technical aspect seems to currently limit the precision of our resonant PEC tuning in the cycle mode, it is absent in the continuous tuning mode. Simple developments should hence allow improving the (already high) precision shown in the main text.

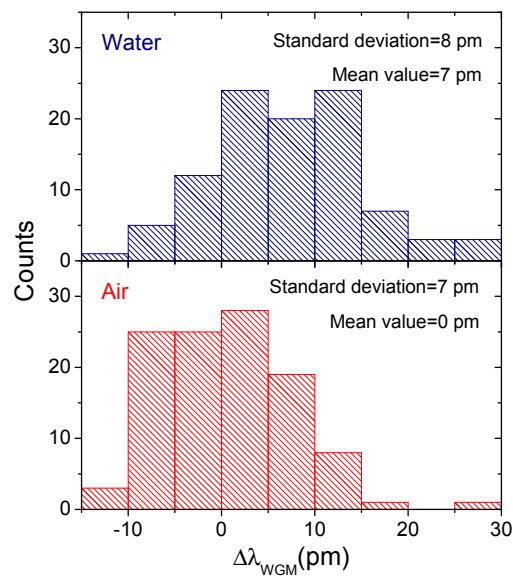


Fig. S2. Laser and tuning precision. Upper panel: Histogram of the measured wavelength shift per cycle in water, built from a series of one hundred cycles of resonant PEC tuning. Lower panel: the same histogram is obtained from measurements performed in air, where PEC etching occurs with 6 orders of magnitude less intensity.

Resonant cavity-enhanced PEC tuning of three cavities

Supplementary Figures S3 and S4 provide supplementary data on the collective PEC tuning of three detuned GaAs resonators. Supplementary Figure S3 shows the set of three disk resonators, imaged at different scales, in order to allow visibility of the optical coupling waveguide, and visualizing the immersion in a droplet of liquid water. Supplementary Figure S4 shows a series of nine optical spectra acquired on a set of three distinct disks placed around the same optical coupling waveguide, in the configuration shown in Supplementary Figure S3.

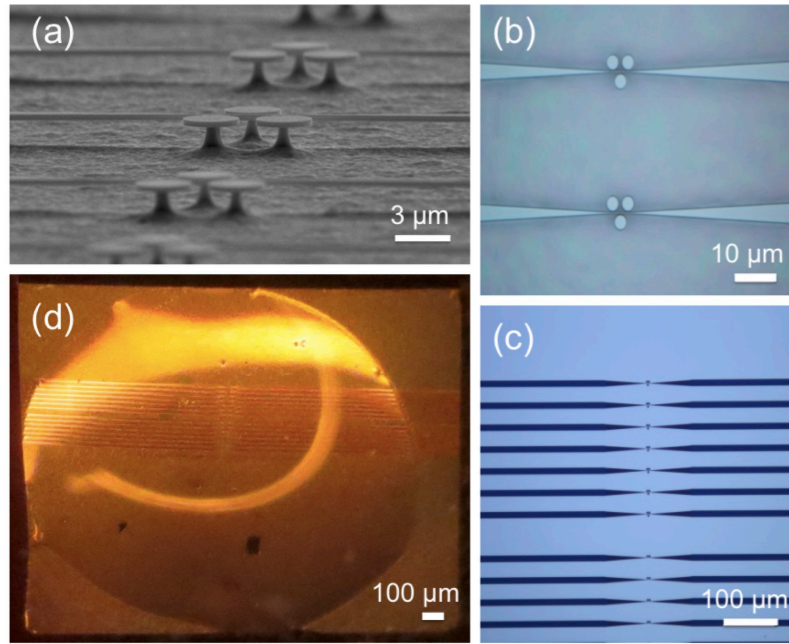


Fig. S3. Three GaAs disk resonators on a chip. (a) Side-view electron micrograph of sets of 3 disks positioned on both sides of a common GaAs suspended optical-coupling waveguide. (b) Top-view optical micrograph of similar sets, with the tapering of the waveguide made visible. (c) Top-view optical micrograph of the waveguides. (d) Top-view optical micrograph of the chip immersed in a liquid droplet.

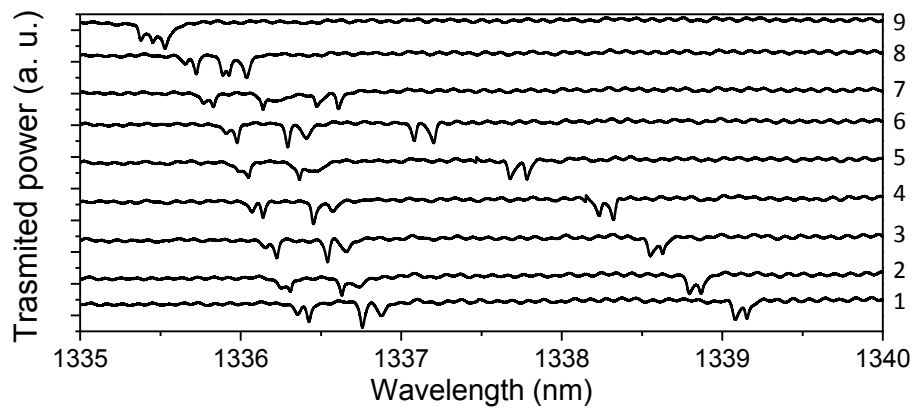


Fig. S4. Collective tuning of three photonic resonators by resonant PEC etching in liquid water. Optical spectra corresponding to step-by-step spectral alignment of three WGM resonators in the configuration shown in Fig. S3. Each doublet corresponds to one disk to start with.

Residual non-selective PEC tuning of cavities

As visible in the data of Fig. 4 (top panel), there is a residual non-selective etching that takes place in our tuning experiments, at least in the “sweep-cycle” mode. Its amplitude varies from one experimental situation to another. In Fig. 4 (top), it happens to be pretty large (about 4nm). In Fig. S4, it is more moderate (less than 1 nm). Here we clarify the origin of this residual non-selective etch and discuss how it can be controlled in future experiments.

We have identified 3 sources of residual non-selective etching:

a- First, it is little known but GaAs gets (very) slowly etched in water. This means that even in the absence of light, a GaAs photonic resonator immersed in water changes dimensions and experiences a slow drift of its resonances. The very small amount of matter dissolved makes it hardly measurable, but an etch speed of 36 pm/min is reported in [1]. We measured the shift of our GaAs disks WGM resonances in water without light, during several tens of minutes, and deduced an etch speed of 42 ± 8 pm/min, which for a $1 \mu\text{m}$ radius disk is also the amount of WGM wavelength shifting. This value is consistent with the extrapolation at zero power of the power-dependent data shown in Fig. 2d of main text. In consequence, in order to limit the amount of non-specific etching in the liquid, one shall first limit the duration of PEC tuning operations. In the present report, this aspect is not optimized at all; hence some residual non-selective etching is taking place in water. In humid air, the phenomenon is reduced a lot (we estimated a difference of about 6 orders of magnitude in the etching speed between water and ambient humid air, see main text).

b- Second, even when laser light is resonantly injected into the WGM of a first disk (Disk 1), while detuned from the WGM resonance of another disk (Disk 2), there is still some optical power dropped into that second disk. This undesired power decreases when the Q of resonances increases, or when the detuning between both WGM resonances increases, but it must be accounted for. In Fig. S5, we have calculated the ratio between the powers circulating in Disk 1, Disk 2 and in their common coupling waveguide, in a configuration where the disk/guide evanescent coupling conditions are equal for both disks, with a contrast of the WGM resonance of 0.7 and a loaded Q of 22,000 (black curve) or 220,000 (blue curve). The laser is exactly resonant with the WGM of Disk 1 and detuned from that of Disk 2 by a wavelength detuning $\Delta\lambda$. For the loaded Q of 22,000, this configuration is basically that of the experiments reported in Fig. 4 of main text (top panel). The case with loaded Q of 220,000 illustrates the trend when Q increases. The calculations are done for a varying detuning, and are based on the standard coupled-mode-theory treatment of disk/guide configurations.

For a detuning $\Delta\lambda=1\text{nm}$, the circulating power in Disk 2 is 10^{-3} of that in Disk 1 (for a Q of 22,000), implying a difference of the same factor in the PEC etching rates. Hence a disk-to-disk PEC tuning selectivity of 10^3 is expected at a spectral distance of 1 nm in the experiments of Fig. 4 (top panel). In the collective PEC tuning, this selectivity progressively drops when the two disks merge spectrally, until they are perfectly aligned.

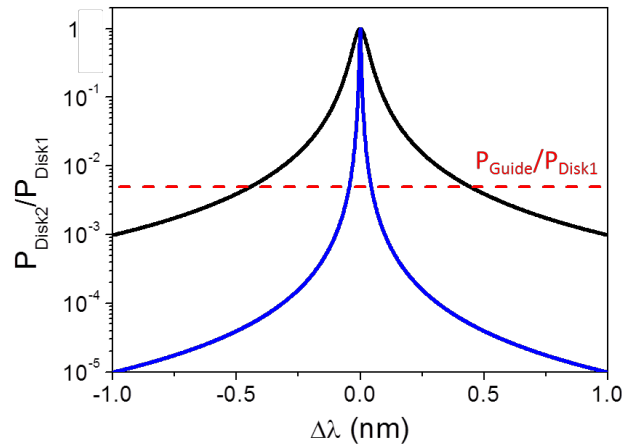


Fig. S5. Relative optical powers circulating in two disks whose WGMs are detuned by $\Delta\lambda$ and are addressed by the same waveguide. The WGM of Disk 1 is resonantly pumped by the laser and the disk/waveguide evanescent coupling conditions are the same for both disks. The loaded Q is 22,000 (blue) or 220,000 (black), with a resonance contrast of 0.7.

c- Third, even when the laser is largely detuned from any WGM resonance, such that zero power is dropped into any disk, there is still light travelling in the waveguide. Hence in liquid a (non-resonant) PEC etching occurs at the guide’s interfaces, reducing its dimensions. Because the guide sits in the evanescent part of the WGM modes and dispersively acts on them, the WGM resonances are blue-shifted by

this etching. Electromagnetic numerical simulations can evaluate this effect. In the experimental conditions of Fig. 4 (top panel), they show that etching 1 nm in the lateral dimensions of the waveguide produces a blue shift of the WGM wavelength of 5 pm. In comparison, etching 1 nm in the radius of the disk produces a WGM shift of 1 nm. Relatively, the effect of waveguide etching is 200 times smaller. We carried out supplementary in-liquid experiments with 20 μ W of optical power travelling in the waveguide, during few tens of minutes and in a largely detuned configuration, and measured a WGM wavelength shifting of 75 pm/min. Knowing the contribution due to water etching without light, we deduce 33 ± 8 pm/min of WGM shifting due to non-selective waveguide etching, at this specific optical power. This is commensurable with the amount of water-induced etching without light. At the smaller optical power generally employed in our tuning experiments, this waveguide contribution is however greatly reduced.

With all these elements at hand, we can establish a hierarchy in the mechanisms of non-selective PEC tuning observed in the top panel of Fig. 4, in the sweep-cycle tuning mode. At $\Delta\lambda=1$ nm, the power circulating in the waveguide is 5 times larger than in Disk 2 (see Fig. S5), but since the waveguide etching has relatively 200 times less influence on WGM resonance shifting, the tuning due to waveguide etching is finally 40 times smaller than that due to etching of Disk 2. For the same $\Delta\lambda=1$ nm, the tuning due to etching of Disk 2 is a factor 1000 smaller than the selective tuning of Disk 1. However finally in Fig. 4 (top panel), the measured selectivity is far from such a factor 1000, which indicates that the slow etching of GaAs in water (without light) must be responsible for most of the non-specific tuning. In Fig. 4 (top panel), the “sweep-cycle” tuning mode was employed and no specific attention was paid to reduce the time interval between subsequent tuning cycles and acquisitions of spectra, generating unnecessary exposure to water and a sizable non-specific etching.

We further support this analysis by looking at another set of data taken in similar conditions, but on two resonators instead of five. In Fig. S6, we control more precisely the duration of each tuning step (2 min per step). The power travelling in the waveguide is 2 μ W. According to our previous analysis, at this power WGM shifting due to waveguide etching becomes $3,3 \pm 1$ pm/min, hence a blue shift of $6,6 \pm 2$ pm per 2-minute cycle. Concomitantly, the water etching without light produces a blue shift of 84 ± 16 pm in 2 minutes, which is more than 10 times larger. Over the total of 6 cycles shown below, these two mechanisms produce overall a non-selective shift of 504 ± 96 pm, which is indeed what is observed in Fig. S6.

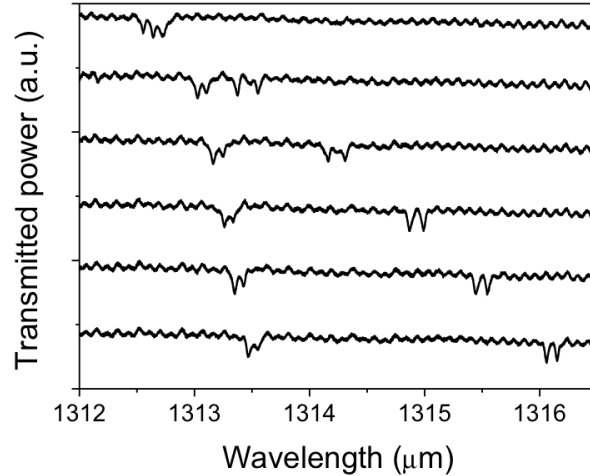


Fig. S6. Resonant PEC tuning of two GaAs disk resonators in water, in the sweep-cycle tuning mode. The duration of each cycle, between two spectrum acquisitions, is controlled to be reproducibly 2 minutes.

In conclusion, in our current in-water PEC tuning experiments in the “sweep-cycle” tuning mode, the slow etching of GaAs in water in the absence of light is dominantly responsible for the non-specific tuning, and has currently limited our selectivity to a value of about 100 at best for conditions similar to those of Fig. 4 (top panel). Using the continuous-tuning mode instead of sweep-cycles, operating in a gas atmosphere of controlled humidity, and using larger Q_s , will all allow mitigating this non-specific tuning and further increase the selectivity.

Resonant PEC tuning of two cavities in humid air

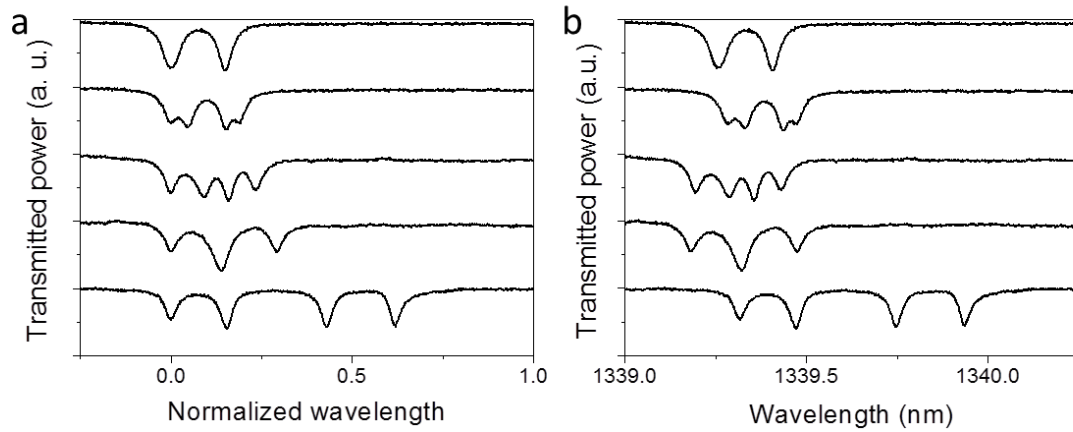


Fig. S7. a) Resonant PEC tuning of two cavities in humid air. The data of Fig. 4 top panel are completed with intermediate steps. b) The same tuning series is shown, without renormalization of the relative detuning. This illustrates the spectral wandering taking place in this long (several hours) tuning procedure, which is a consequence of temperature variations in the laboratory.

References

1. S. Sioncke, D. P. Brunco, M. Meuris, O. Uwamahoro, J. Van Steenberghe, E. Vrancken, and M. M. Heyns. Etch rates of Ge, GaAs and InGaAs in acids, bases and peroxide based mixtures. ECS Transaction, 16 (10), 451- 460 (2008)